

# ChemComm

Accepted Manuscript



This is an *Accepted Manuscript*, which has been through the Royal Society of Chemistry peer review process and has been accepted for publication.

*Accepted Manuscripts* are published online shortly after acceptance, before technical editing, formatting and proof reading. Using this free service, authors can make their results available to the community, in citable form, before we publish the edited article. We will replace this *Accepted Manuscript* with the edited and formatted *Advance Article* as soon as it is available.

You can find more information about *Accepted Manuscripts* in the [Information for Authors](#).

Please note that technical editing may introduce minor changes to the text and/or graphics, which may alter content. The journal's standard [Terms & Conditions](#) and the [Ethical guidelines](#) still apply. In no event shall the Royal Society of Chemistry be held responsible for any errors or omissions in this *Accepted Manuscript* or any consequences arising from the use of any information it contains.



ChemComm

COMMUNICATION

## Nanofibrous Microspheres via Emulsion Gelation and Carbonization†

Received 00th January 20xx,  
Accepted 00th January 20xx

Xia Liu,<sup>a,b,c</sup> Adham Ahmed,<sup>c</sup> Zhenxin Wang,<sup>\*a</sup> and Haifei Zhang<sup>\*c</sup>

DOI: 10.1039/x0xx00000x

www.rsc.org/

**Nanofibrous hydrogel microspheres are formed by pH gelation of perylene diimide derivatives in emulsion droplets. These microspheres are freeze-dried and subsequently carbonized to produce discrete N-doped nanofibrous carbon microspheres. The carbon microspheres show high performance as electrode materials for supercapacitor.**

Carbon-based materials with different micro- or nano-structures, including fullerenes, single- and multi-walled carbon nanotubes, graphene, and carbon nanofibers (CNFs), are promising materials for electrochemical energy storage.<sup>1,2</sup> Carbon materials may be prepared in the format of spheres with N-doping for improved electrochemical applications.<sup>3,4</sup> Carbon microspheres with homogeneous packing can reduce the diffusion resistance. The interstitial voids between the microspheres allow easy access of the electrolyte to the electrodes, hence to improve the performance.<sup>5,6</sup> Porous carbon microspheres and nanospheres can be prepared by various approaches.<sup>3</sup> However, there have been few reports on the preparation of nanofibrous carbon spheres. Nanofibers of polymer, carbon, and composites are extensively prepared by electrospinning (although other methods available as well), which have found wide applications in tissue engineering, separation, and energy applications.<sup>7,8</sup> However, it is extremely difficult to prepare such nanofibrous spheres by the electrospinning approach. Other approaches such as chemical vapor deposition or catalytic gas deposition approach to prepare carbon nanofibers can be equally difficult to form nanofibrous carbon microspheres.<sup>8,9</sup> As carbon can be prepared by carbonization of carbon-rich polymer, we hypothesize that nanofibrous carbon-rich organic/polymeric microspheres may be prepared first and then followed by carbonization.

Although there are a lot of reports on the preparation of polymer or organic microspheres, they are usually porous but not nanofibrous.<sup>10</sup> Only a few reports have been found in literature on formation of nanofibrous polymeric microspheres. These include nanofibrous collagen microspheres by collagen reconstitution,<sup>11</sup> chitin microspheres by thermally induced gelation,<sup>12</sup> hollow and novel microspheres from star-shaped poly(L-lactic acid) by thermally induced phase separation (TIPS).<sup>13</sup> All these reports involve emulsification and gelation/phase separation in the droplet phase of the emulsions. These nanofibrous microspheres have been used to deliver proteins or to support cell growth.<sup>11-13</sup> It is possible to form nanofibrous poly(L-lactic acid) microsphere from its dimethylformamide solution via varying concentrations by TIPS but there is limited control on microsphere morphology.<sup>14</sup> We report here the preparation of nanofibrous microsphere from the carbon-rich perylene diimide derivatives by pH-triggered gelation in emulsion droplet phase. The freeze-dried microspheres are then carbonized to produce nanofibrous carbon microspheres for the first time (Fig. 1), which are evaluated as high performance electrode material for supercapacitors.

Perylene diimides (PDIs) are primarily soluble in organic solvents. Due to their quadrupolar  $\pi$  system and  $\pi$ - $\pi$  stacking nature in self-assembled structures, PDIs have been extensively investigated for applications such as biosensing, light emitting diodes, field effect transistors and photovoltaic cells.<sup>15,16</sup> Recently, investigation of water soluble perylene diimides has intensified, by modification of perylene diimide molecules to provide ionic substituents at the imide positions and/or bay positions.<sup>17</sup> Once dissolved in water, the gelation/self-assembly of such perylene diimide derivatives may be initiated conveniently by change of pH or crosslinking with melamine.<sup>17-19</sup> Particularly, the modified PDIs with amino acids can form homogeneous gels by the controlled hydrolysis of glucono- $\delta$ -lactone (GdL) to gradually reduce the solution pH.<sup>20</sup>

In this study, perylene-3,4,9,10-tetracarboxylic dianhydride was firstly reacted with 5-aminoisophthalic acid to produce a PDI derivative with four carboxylic group (PDI-COOH) (Fig. 1).<sup>16</sup> As depicted in Fig 1, this molecule is dissolved in basic water with GdL and then emulsified into an oil phase to produce a water-in-oil

<sup>a</sup> State Key Laboratory of Electroanalytical Chemistry, Changchun Institute of Applied Chemistry, Chinese Academy of Sciences, 5625 Renmin Street, Changchun 130022, P. R. China. E-mail address: wangzx@ciac.ac.cn

<sup>b</sup> University of Chinese Academy of Sciences, Beijing 100039, P. R. China.

<sup>c</sup> Department of Chemistry, University of Liverpool, Oxford Street, Liverpool L69 7ZD, United Kingdom. E-mail address: zhanghf@liv.ac.uk

† Electronic Supplementary Information (ESI) available: [details of any supplementary information available should be included here]. See DOI: 10.1039/x0xx00000x

(W/O) emulsion. The hydrolysis of GdL in the aqueous droplet phase triggers the gelation of PDI-COOH. Due to the high carbon content in PDI-COOH molecules, the gel microspheres may be easily carbonized to produce nanofibrous carbon microspheres.

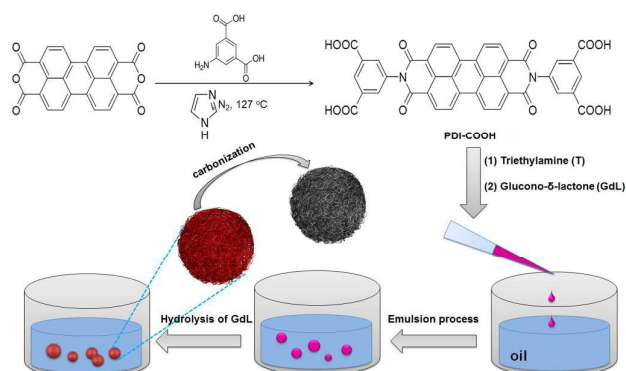


**Fig. 1** Schematic illustration showing the synthesis process of PDI-COOH and the emulsification process (water-in-oil emulsion) for the fabrication of nanofibrous carbon microspheres.

PDI-COOH is not soluble in neutral water but can be dissolved in basic water. It is fine to use NaOH as the base but this may introduce additional Na into the final carbonized materials. We have therefore chosen an organic base triethylamine (TEA). PDI-COOH was dissolved in basic aqueous solution with the molar ratio of PDI-COOH:TEA = 1:6, which was then emulsified into *o*-xylene in the presence of Span-80 (a sorbitan monooleate surfactant with HLB value of 4.3, known to stabilize W/O emulsions).<sup>21</sup> *o*-xylene was chosen as the oil phase due to its low vapour pressure and low toxicity.<sup>22</sup> The emulsion droplets with a diameter of approximately 50  $\mu\text{m}$  could be obtained. To initiate gelation in the droplets, 26  $\text{mg cm}^{-3}$  GdL was added into the PDI-COOH solution before emulsification. With the emulsion formed and hydrolysis of GdL in the aqueous droplets, the decreased pH induced the self-assembly and gelation of PDI-COOH, resulting into the formation of nanofibrous gel microspheres.

The concentration of PDI-COOH solution was very important to produce stable nanofibrous microspheres. At the concentration of 20 mM, relatively uniform red microspheres with diameters of *ca.* 50  $\mu\text{m}$  were formed (Fig. S1a, ESI<sup>†</sup>). After freeze-drying, separated particles with patched surface were obtained (Fig. S1b, ESI<sup>†</sup>). The scanning electron microscopic (SEM) imaging at high magnification showed the particles were constructed of entangled nanofibers with diameters of *ca.* 50 nm (Fig. S1c, ESI<sup>†</sup>). When the concentration of PDI-COOH decreased to 10 mM, nanofibrous particles with similar morphologies were still formed (Fig. S1d-f, ESI<sup>†</sup>). However, further reducing the concentration to 5 mM, the particles collapsed into capsule shells, with the nanofibers tending to aggregate (Fig. S1g-i, ESI<sup>†</sup>).

It is believed that the emulsion stability might influence significantly the gelation in droplet phase and the formation of gel microspheres. 5 mM PDI-COOH solution was used to investigate this potential impact. Polystyrene of different molecular weights (MWs) was dissolved in *o*-xylene to increase the viscosity and improve the emulsion stability. Discrete microcapsules with densely

positioned nanofibers were obtained from the emulsion containing polystyrene (MW 35K) (Fig. S2d-f, ESI<sup>†</sup>). With the increasing molecular weight of polystyrene (MW 192K, termed as PS192), uniform microspheres (rather than with patched surface) were formed with the nanofibrous morphology (Fig. S2g-i, ESI<sup>†</sup>). But the nanofibers were not uniformly distributed and the nanofibrous microspheres seemed loose. It was reported that addition of salt could improve the emulsion stability.<sup>23</sup> When 0.5 M NaCl was added into aqueous solution, more uniform nanofiber structure was observed from the freeze-dried microspheres (Fig. S2j-l, ESI<sup>†</sup>). In addition, different concentrations of Span 80 (5–50 wt%, Fig. S3, ESI<sup>†</sup>) and PS192 (5–15 wt%, Fig. S4, ESI<sup>†</sup>) were studied. The optical images demonstrated that the formed hydrogel microspheres were more uniform and stable with increasing the concentration of Span 80. The solubility of PS192 was limited in the *o*-xylene with 50% Span 80 and the concentration effect was not obvious.

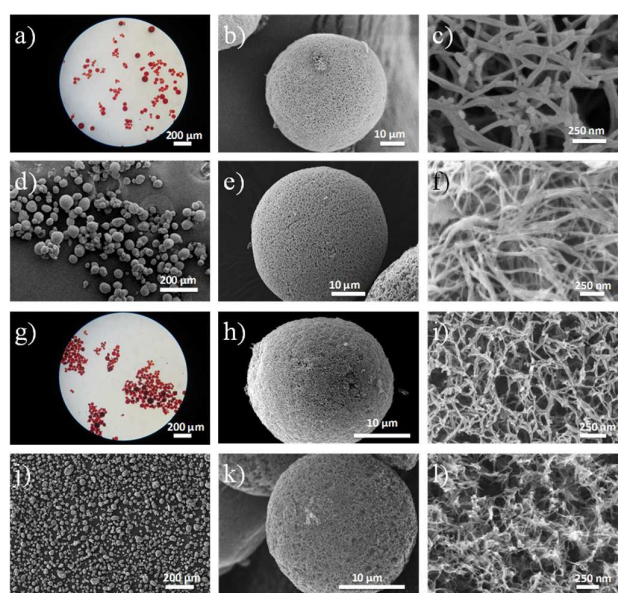


**Fig. 2** The optical and SEM images of nanofibrous hydrogel and carbon microspheres. The microspheres prepared from TEA + GdL precursors: the optical image of hydrogel microspheres (a), SEM micrographs of the freeze-dried microspheres (b-d) and the carbonized microspheres (e, f). The microspheres prepared from TEA + MM + F-127 + GdL precursors: the optical image of hydrogel microspheres (g), SEM micrographs of the freeze-dried microspheres (h-i) and the carbonized microspheres (j-l). All samples were prepared using optimized condition: 20 mM PDI-COOH solution and 40 mM MM (in 0.05  $\text{mg cm}^{-3}$  F-127 solution) using the volume ratio of water phase/oil phase (1/8) to form the water-in-oil emulsion, containing 50% span 80, 10% polystyrene (MW 192K) and 1.25% 0.5 M NaCl.

High PDI-COOH concentration (20 mM) and use of PS192 (10 wt%) with 50 wt% Span-80 were then combined in order to produce mechanically stable nanofibrous microspheres. With the volume ratio of water phase:oil phase remained at 1:4, some microspheres with broken pieces were formed (Fig. S5a, b, ESI<sup>†</sup>). Different ratios of water to oil were investigated (Fig. S5, ESI<sup>†</sup>). Fine microspheres with nanofibrous structures were generated at the water:oil ratio of 1:8 (Fig. S5c-d, ESI<sup>†</sup>). However, the size distribution of the

microspheres was broad. NaCl solution was then introduced to further improve the microsphere morphology, which produced the best hydrogel microspheres under our preparation conditions (Fig. 2a-d). The red hydrogel microspheres could be easily collected by centrifuging the emulsion and then redispersed into ethanol, acetone and cyclohexane for washing. After freeze-drying, the nanofibrous dry microspheres maintained the spherical shape and uniformly distributed nanofibers (Fig. 2a-d). Further carbonization of these microspheres under nitrogen produced nanofibrous carbon spheres with the sizes of the microspheres ( $\sim 50 \mu\text{m}$ ) and the nanofibers ( $\sim 50 \text{nm}$ ) largely unchanged (Fig. 2e-f).

The preparation of nanofibrous microspheres included the gelation of PDI-COOH molecules in the emulsion droplets and the subsequent freeze-drying of the collected microspheres. The nanofibers were formed during the gelation in droplets, resulting from the self-assembly of PDI-COOH molecules into 1D nanostructure with the diameter of discrete nanofibers  $\sim 20 \text{nm}$ . This was due to the hydrogen bonding between protonated carboxylic acids and  $\pi$ - $\pi$  stacking interaction among the perylene cores.<sup>16,17,24</sup> However, when the gel was air dried, dense and aggregated nanofibers were formed.<sup>16</sup> The freeze drying process helped to maintain the porous microspheres structure and limit the aggregation of the discrete gel nanofibers.

This procedure was further used to produce N-doped carbon microspheres. Melamine (MM), a molecule with high N content, was used to crosslink PDI-COOH molecules by dissolving MM in the aqueous PDI-COOH solution before emulsification.<sup>16</sup> However, irregular and broken particles were formed, and the nanofibers were somewhat aggregated (Fig. S6a-d, ESI<sup>†</sup>). Based on our observation, it was believed that melamine with high concentration could precipitate out during the gelation process due to limited solubility, which made the emulsion unstable. A block copolymer Pluronic F-127 was added to improve the preparation, because that (1) it could help dissolve melamine; (2) it could produce N-doped carbon microspheres with additional surfactant templated pores. F-127 was dissolved in MM solution and then mixed with the PDI-COOH solution. The nanofibrous carbon microspheres (NCM) prepared with MM + F-127 were termed as NCM-MF, while the ones prepared with M only termed as NCM-M. The introduction of MM + F-127 in the emulsion droplet phase led to smaller gel microspheres and finer nanofibers ( $\sim 20 \text{nm}$ ) (Fig. 2g-i). The polymer F-127 was removed simultaneously during carbonization. After carbonization, the structure of microsphere and nanofiber was well retained (Fig. 2j-l).

Powder X-ray diffraction (PXRD) analysis revealed a broad peak at  $2\theta$  values of  $24^\circ$  for the carbon microsphere samples (Fig. S7), attributing to the (002) reflections of turbostratic carbon structure. Raman spectroscopy showed two overlapping peaks at  $1350 \text{cm}^{-1}$  and  $1580 \text{cm}^{-1}$  (Fig. S8), corresponding to the  $A_{1g}$  mode (disordered carbon structure, D-band) and the  $E_{2g}$  mode (C=C stretching in graphitic carbon, G-band). The ratio of the intensity of G- and D-band,  $I_G/I_D$ , was found to be 0.96, 0.99, and 1.03 for NCM, NCM-M and NCM-MF, respectively. This indicates a disordered turbostratic carbon structure for all carbon microspheres but slightly improved graphitic content for NCM-MF. X-ray photoelectron spectroscopy (XPS) analysis showed increasing intensity of N signals for NCM, NCM-M and NCM-MF, with a relatively high amount of quaternary

nitrogen (Fig. S9, ESI<sup>†</sup>). The N content of 4.69% (atomic percentage) was confirmed for the NCM-MF spheres. Although XPS is a surface characterization technique, this value should reflect the N content in the bulk material if N is uniformly distributed in the material. The elemental microanalysis gave a N content of 3.61% for the NCM-MF (2.52% for NCM and 3.26% for NCM-M). The Brunauer-Emmett-Teller (BET) surface areas of NCM, NCM-M and NCM-MF by  $\text{N}_2$  sorption were  $303 \text{m}^2 \text{g}^{-1}$ ,  $431 \text{m}^2 \text{g}^{-1}$  and  $427 \text{m}^2 \text{g}^{-1}$ , respectively (Fig. S10, Table S1). Such surface areas are quite good for carbon nanofibers.<sup>9</sup> Addition of MM during the gelation increased the surface area for carbon microspheres while F-127 templating has increased the micropore area and volume considerably (Table S1). The macropores of the nanofibrous microspheres were characterized by Hg intrusion porosimetry. It gave similar macropore size distribution, with two peaks around  $1.6 \mu\text{m}$  (voids between the nanofibers in the microspheres) and  $90 \mu\text{m}$  (voids between the microspheres) (Fig. S11, ESI<sup>†</sup>). The intrusion volumes were  $10.43 \text{cm}^3 \text{g}^{-1}$  for NCM-MF and  $11.46 \text{cm}^3 \text{g}^{-1}$  for NCM-M, indicating highly porous and light carbon microspheres.

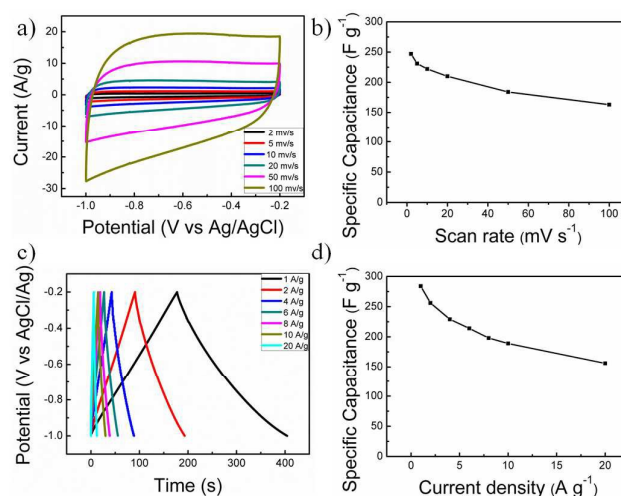


**Fig. 3** Electrochemical evaluation of the NCM-MF carbon microspheres. Cyclic voltammograms using different scan rates (a), variation of specific capacitance with scan rate (b), Galvanostatic charge/discharge curves at different current densities (c) and variation of specific capacitance with current density (d). All the tests were carried out in 6 M aqueous KOH solution in the voltage window of  $-1.0 \text{V} - -0.2 \text{V}$ . The NCM-MF slurry was coated on Ni foam as working electrode, Pt sheet as counter electrode, and Ag/AgCl electrode as reference electrode.

The nanofibrous carbon microspheres prepared in this study were evaluated as an electrode material for supercapacitors, by cyclic voltammetry (CV) and galvanostatic charge/discharge techniques using a three-electrode system. The microsphere dispersion in ethanol was dropped on a piece of Ni foam ( $1 \times 1 \text{cm}^2$ ) and then used as working electrode with a loading of about  $1 \text{mg cm}^{-2}$ . At the same scan rate, the increasing capacitance was observed for NCM < NCM-M < NCM-MF electrodes (Table S2). Fig. 3a shows that the CV curves of NCM-MF are nearly rectangular, indicating good charge propagation within the electrode. The shape of the CV curves changed slightly even when the scan rate increased

to 100 mV s<sup>-1</sup>, indicating a quick charge propagation capability of both double layer capacitances (Fig. 3a). The capacitance decreased with the increase of scan rate (Fig. 3b). Similar shapes of CV curves and trend of capacitance were observed for NCM and NCM-M, but with lower capacitance (Fig. S12, Table S2). A capacitance of 247 F g<sup>-1</sup> at 2 mV s<sup>-1</sup> and 163 F g<sup>-1</sup> at 100 mV s<sup>-1</sup> were recorded. In contrast, the capacitance for NCM and MCM-M was much lower, 12 F g<sup>-1</sup> and 109 F g<sup>-1</sup> at 100 mV s<sup>-1</sup> respectively (Table S2, ESI<sup>†</sup>). This increase in capacitance approximately agrees with the increase of surface area and N content, although not proportionally. The significant increase from NCM-M to NCM-MF may be attributed to the considerably increased microporosity in NCM-MF (Table S1). The rate performance of NCM-MF electrode was evaluated by galvanostatic charge/discharge at different current densities (Fig. 3c). The specific capacitance was gradually reduced with the increasing current density (Fig. 3d). The specific capacitance remained above 200 F g<sup>-1</sup> at the current density of 6 A g<sup>-1</sup> (Table S2, ESI<sup>†</sup>), which showed greater or comparable discharge capacity compared to relevant carbon nanofibers.<sup>25-26</sup> The superior performance of the NCM-MF electrode was also confirmed by impedance spectroscopy (Fig. S13), indicating the decreased interfacial charge-transfer resistance. Furthermore, the NCM-MF showed the smallest internal resistance determined by IR drop from the charge/discharge curves (Fig. S14). This NCM-MF electrode had good stability as confirmed by galvanostatic charge/discharge measurements at a current density of 4 A g<sup>-1</sup>. The specific capacitance remained at a high value of 150 F g<sup>-1</sup> after 1000 cycles (Fig. S15, ESI<sup>†</sup>). Overall, the superior performance of the NCM-MF electrode may be attributed to the combination of fine nanofibers, higher microporosity, N-doping, and increased graphitic content in NCM-MF.<sup>25-29</sup>

## Conclusions

A novel one-pot synthesis strategy to prepare nanofibrous microsphere using W/O emulsion via pH-triggered gelation of perylene diimide derivatives has been demonstrated. These microspheres can be pyrolyzed under N<sub>2</sub> to produce nanofibrous carbon microspheres. Melamine and F-127 can be introduced to generate N-doped and templated carbon microspheres with the nanofiber diameter around 20 nm. The nanofibrous carbon microspheres are evaluated as electrode for supercapacitor, showing a high specific capacitance of 284 F g<sup>-1</sup> at a current density of 1 A g<sup>-1</sup>, 214 F g<sup>-1</sup> at 6 A g<sup>-1</sup>, and good rate capability with the specific capacitance remaining at 67% after 1000 cycles at current density of 4 A g<sup>-1</sup>.

XL acknowledges the joint PhD studentship from China Scholarship Council. The authors are grateful for the access to the facilities in the Centre for Materials Discovery at the University of Liverpool. ZW thanks the NSFC (Grant No.21127010) and Jilin Provincial Science and Technology Department (Grant No. 20100701) for financial supports.

## Notes and references

- H. Nishihara and T. Kyotani, *Adv. Mater.*, 2012, **24**, 4473.
- S. Nardecchia, D. Carriazo, M. L. Ferrer, M. C. Gutiérrez and F. del Monte, *Chem. Soc. Rev.*, 2013, **42**, 794.
- P. Zhang, Z. Qiao, S. Dai, *Chem. Commun.*, 2015, **51**, 9246.
- N. P. Wickramaratne, J. Xu, M. Wang, L. Zhu, L. Dai and M. Jaroniec, *Chem. Mater.*, 2014, **26**, 2820.
- A. A. Deshmukh, S. D. Mhlanga and N. J. Coville, Carbon spheres, *Mater. Sci. Eng. R-Rep.*, 2010, **70**, 1.
- Q. Li, R. Jiang, Y. Dou, Z. Wu, T. Huang, D. Feng, J. Yang, A. Yu and D. Zhao, *Carbon*, 2011, **49**, 1248.
- Q. P. Pham, U. Sharma, A. G. Mikos, *Tissue Eng.*, 2006, **12**, 1197.
- M. Inagaki, Y. Yang, F. Kang, *Adv. Mater.*, 2012, **24**, 2547.
- J. K. Chinthaginjala, K. Seshan, L. Lefferts, *Ind. Eng. Chem. Res.*, 2007, **46**, 3968.
- J.-B. Fan, C. Huang, L. Jiang and S. Wang, *J. Mater. Chem. B*, 2013, **1**, 2222.
- O. Chan, K.-F. So and B. Chan, *J. Controlled Release*, 2008, **129**, 135.
- B. Duan, X. Zheng, Z. Xia, X. Fan, L. Guo, J. Liu, Y. Wang, Q. Ye and L. Zhang, *Angew. Chem. Int. Ed.*, 2015, **54**, 5152.
- Z. Zhang, R. L. Marson, Z. Ge, S. C. Glotzer and P. X. Ma, *Adv. Mater.*, 2015, **27**, 3947.
- M. Liu, Y. Liu, R. Liu, F. Wei and R. Xiao, *J. Mater. Chem. A*, 2015, **3**, 14054.
- L. Schmidt-Mende, A. Fechtenkötter, K. Müllen, E. Moons, R. H. Friend and J. MacKenzie, *Science*, 2001, **293**, 1119.
- P. K. Sukul, D. Asthana, P. Mukhopadhyay, D. Summa, L. Muccioli, C. Zannoni, D. Beljonne, A. E. Rowan and S. Malik, *Chem. Commun.*, 2011, **47**, 11858.
- D. Görl, X. Zhang and F. Würthner, *Angew. Chem. Int. Ed.*, 2012, **51**, 6328.
- A. Datar, K. Balakrishnan and L. Zang, *Chem. Commun.*, 2013, **49**, 6894.
- E. R. Draper, J. J. Walsh, T. O. McDonald, M. A. Zwiijnenburg, P. J. Cameron, A. J. Cowan and D. J. Adams, *J. Mater. Chem. C*, 2014, **2**, 5570.
- D. J. Adams, M. F. Butler, W. J. Frith, M. Kirkland, L. Mullen and P. Sanderson, *Soft Matter*, 2009, **5**, 1856.
- S.D. Kimmins, N.R. Cameron, *Adv. Funct. Mater.*, 2011, **21**, 211.
- N. Grant and H. Zhang, *J. Colloid Interface Sci.* 2011, **356**, 573.
- V. Rajagopalan, C. Solans and H. Kunieda, *Colloid Polym. Sci.*, 1994, **272**, 1166.
- A. Datar, K. Balakrishnan and L. Zang, *Chem. Commun.*, 2013, **49**, 6894.
- L. F. Chen, Z. H. Huang, H. W. Liang, H. L. Gao and S. H. Yu, *Adv. Funct. Mater.*, 2014, **24**, 5104.
- V. Barranco, M. Lillo-Rodenas, A. Linares-Solano, A. Oya, F. Pico, J. Ibañez, F. Agullo-Rueda, J. Amarilla and J. Rojo, *J. Phys. Chem. C*, 2010, **114**, 10302.
- L. F. Chen, X. D. Zhang, H. W. Liang, M. Kong, Q. F. Guan, P. Chen, Z. Y. Wu and S. H. Yu, *ACS Nano*, 2012, **6**, 7092.
- L. Zhao, L. Fan, M. Zhou, H. Guan, S. Qiao, M. Antonietti and M. Titirici, *Adv. Mater.* 2010, **22**, 5202.
- H. Ji, X. Zhao, Z. Qiao, J. Jung, Y. Zhu, Y. Lu, L. L. Zhang, A. H. MacDonald and R. S. Ruoff, *Nature Commun.* 2014, **5**:3317.